Journal of Materials Processing Technology 210 (2010) 1918–1925

Contents lists available at ScienceDirect

Journal of Materials Processing Technology

journal homepage: www.elsevier.com/locate/jmatprotec

Pulsed Nd:YAG laser cutting of NiTi shape memory alloys—Influence of process parameters

Ronny Pfeifer*, Dirk Herzog, Michael Hustedt, Stephan Barcikowski

Laser Zentrum Hannover e.V., Hollerithallee 8, 30419 Hannover, Germany

ARTICLE INFO

Article history:
Received 16 February 2010
Received in revised form 25 June 2010
Accepted 2 July 2010

Keywords:
Laser
Nd:YAG
Pulsed
Cutting
SMA
Nitinol

ABSTRACT

Shape memory alloys (SMAs), in particular Nitinol (NiTi), are of increasing interest in research and industry due to their outstanding properties, e.g. the shape memory effect (SME) and high biocompatibility. Obviously, it is necessary to machine these elements from NiTi sheet materials using suitable processing methods that provide high precision and retain the shape memory effect. Pulsed Nd:YAG laser cutting of 1 mm thick NiTi shape memory alloys for medical applications (SMA-implants) has been investigated. Due to the local energy input only small heat-affected zones (HAZ) occur and the shape memory properties remain. The influence of key parameters like pulse energy, pulse width, and spot overlap on the cut geometry, roughness and HAZ is shown.

1. Introduction

Along with the shape memory effect, i.e. the ability to remember its shape (one-way- and two-way memory effect) or the pseudoplasticity (the ability to accommodate to high elastic deformation), NiTi SMAs have several outstanding properties. These include high mechanical strength, a high efficiency in converting thermal into mechanical energy and an excellent biocompatibility as shown by Shabalovskaya (2002). Especially the latter makes it highly interesting for several applications in the medical field. A broad overview of general applications of NiTi SMAs in the medical field is given by Lipscomb and Nokes (1996) and Feninat et al. (2001). Besides commonly known applications, e.g. wires for minimal invasive surgery or super(pseudo)elastic devices for cardio-vascular systems (e.g. self-expandable stents) as shown by Stoeckel (2000) and by Feninat et al. (2001), it is also utilized in the orthodontic (Peitsch et al., 2007) and in the orthopedic field. Betz et al. (2005) show the application of NiTi staples for treatment of scoliosis, a deformation of the spinal cord. Besides being used in the field of biomedical applications, NiTi SMAs are also utilized for industrial applications, for the aerospace industry and for Micro-Electro-Mechanical Systems (MEMS). Otsuka and Kakeshita (2002) provide an overview of the application of NiTi SMA as couplings, sensors and actuator. The application of NiTi for miniature grippers, micro-valves and pumps is shown in Gupta et al. (2004).

The drawbacks of NiTi SMAs are their high price and high sensitivity to stress, thermal influences and mechanical tension. Especially mechanical machining is very difficult, due to the low thermal conductivity of NiTi SMA and its low elastic modulus. Thus, mechanical machining results in increased wear and tear of the tool, and in a degradation of the machined surfaces, caused by the material's high ductility and its severe strain hardening as shown by Lin et al. (2000).

In contrast, laser technology is an optimal technology for processing NiTi SMA alloys, especially pulsed laser systems. As described by Shanjin et al. (2006), the thermal properties of the material to be machined have a stronger impact on the effectiveness of the cutting process than the mechanical properties, as laser processing is a thermal process. Due to the non-contact, precise and localized energy input of a laser, which has low thermal impact and therefore generates only a small heat-affected zone, it is the most effective method for cutting a NiTi SMA.

Consequently, cutting NiTi SMA using laser radiation has been described in several publications. Yung et al. (2005) describes the laser based micro-cutting of thin SMA sheets (thickness: 350 μm) using a 355 nm Nd:YAG laser for MEMS applications. Debris-free kerfs with small taper angle were achieved. Haferkamp et al. (1999) used ultrashort-laser pulses (nano-second and femtosecond-pulses) for manufacturing micro-instruments made of NiTi wires. It was shown that, compared to longer pulses, e.g. μs-pulses, the

* Corresponding author at: Laser Zentrum Hannover e.V., Materials and Processes, Hollerithallee 8, 30419 Hannover, Germany. Tel.: +49 511 2788 161; fax: +49 511 2788 100.
E-mail address: r.pfeifer@lzh.de (R. Pfeifer).

0924-0136/$ – see front matter © 2010 Elsevier B.V. All rights reserved.
doi:10.1016/j.jmatprotec.2010.07.004

thermal influence on the material can be reduced to a minimum. Femtosecond laser machining of NiTi alloy was also investigated by Huang et al. (2005). In this investigation, grooves were cut in NiTi alloy specimens using a laser wavelength of λ = 775 nm and a pulse width of 150 fs. A small heat-affected layer (50 μm) and low surface roughness (R_a = 0.4 μm) was achieved. Li et al. (2006) show that femtosecond laser machining of metals is still basically a thermal mechanism. The influence of the laser fluence regarding the ablation rate, recast and cut quality, using a 755 nm Ti:sapphire laser, was investigated.

As shown above, primarily short- and ultrashort pulse laser systems are applied in order to machine SMAs. Advantages of these systems are the extreme good quality cut kerf, the small kerf width and the minimization or lack of thermal affects, respectively, of the material processed. Drawbacks can be seen in the high price and the very low ablation rate (Yung et al.). Hence, from the economic aspect, the application of these lasers systems only pays off for components with very high requirements on the cut quality and thermal load or very thin materials (maximum of a few hundred micrometers).

In general, continuous laser systems (e.g. CO_2 lasers, solid state lasers) or pulsed laser systems with a higher average power and pulse width are used in order to machine thicker specimens and to generate bigger components with longer overall cutting length. Fargas et al. (2007) investigated cutting of NiTi sheets (thickness: 0.5 and 1.0 mm) using a continuous wave Nd:YAG laser. High cutting speeds (v = 3–10 m/min), a small HAZ and a minimum roughness of R_z = 60–40 μm at the cutting edge were obtained.

This paper presents the influence of different parameters on the cut quality of comparably thick NiTi sheets for SMA-implants (thickness: 1 mm, overall cutting length: 150 mm) using a pulsed Nd:YAG laser. The wavelength of the infrared radiation emitted by Nd:YAG lasers is one tenth (λ = 1.06 μm) that of CO_2 lasers (λ = 10.6 μm), which are the most popular lasers used for cutting of thicker materials in general. The short wavelength results in less reflection, and therefore in a high absorbance of the radiation, especially if metallic workpieces are used. Thus, even highly reflecting materials can be processed (Thawari et al., 2005). Compared to CO_2 lasers, further advantage can be seen in the flexibility of handling, e.g. guiding the beam through optical fibers.

2. Experimental

2.1. Material

Binary titanium-rich NiTi alloy sheets with a nominal composition of 49.8–50.0 at.% Ni (rest Ti) and a thickness of 1 mm were used in this study. Due to the composition, the material shows a martensitic structure at room temperature. The sheets were straightly annealed and pickled by chemical etching, resulting in a blank, metallic surface. The physical properties are shown in Table 1.

2.2. Set-up

All experiments were carried out using a pulsed Nd:YAG laser (Model: FLS 352 N, LASAG AG, Switzerland). The laser and process specifications are listed in Table 2. Although the type of the gas normally does not influence the process of inert gas cutting of metals, it does play an important role when cutting nitriding materials, e.g. titanium or NiTi SMA. In order to avoid nitriding and the thus released exothermic energy, which again would result in an increased HAZ and thermal impact, as described by Kaplan (2000), the cutting process was subsequently carried out using argon as process gas. The gas pressure was kept constant at 12 bar, as it should be as high as possible in order to eliminate any dross and to strengthen the momentum that is being transferred to the melt film.

Table 1
Properties of Nitinol (Giroux et al., 1996; Yung et al., 2005).

Properties	Unit	Values
Fusion point	°C	1250
Fusion heat	J/cm³	2322
Density	g/cm³	6.45
Thermal conductivity	W/m K	10–18
Thermal diffusivity	cm²/s	0.125
Specific heat	J/kg K	490
Dilatation coefficient	μm/k	
Austenite		11
Martensite		6.6
Young's modulus	GPa	
Austenite		70
Martensite		30–35
Yield strength	MPa	100–130
Tensile strength	MPa	875
Reversible deformation (one-way m. effect)	%	8
Reversible deformation (two-way m. effect)	%	3.2
Corrosion resistance		Very good
Biocompatibility		Very good

Table 2
Process parameters.

Process parameters	Unit	Values
Pulse energy	J	0.3–1.0
Pulse width	ms	0.15–1.5
Pulse frequency	Hz	100
Pulse shape		Nearly rectangular
Cutting speed	mm/s	0–15
Assist gas		Ar
Gas pressure	bar	12
Nozzle diameter	mm	1.5
Nozzle stand-off	mm	0.4
Focal lens	mm	100
Focus position	mm	0 (at the surface)
Focal spot size	mm	0.3

2.3. Characterization

All optical analyses, e.g. kerf analysis and microstructural changes, were performed using an optical microscope (BX60, Olympus) with an attached CCD-camera (DIG 3300) and the free image processing software “ImageJ”. Kerf width measurements on the entry (k_{entry}) and the exit side (k_{exit}) were carried out at 3 different locations (Fig. 1). The heat-affected zone as well as the microstructure of the HAZ were viewed after appropriate metallographic preparation. The specimens were mounted in an epoxy-based resin,

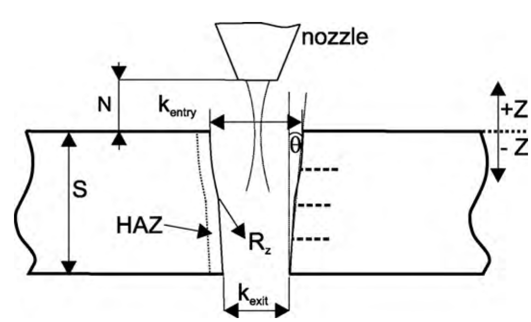

Fig. 1. Schematic illustration of the various cut quality attributes used in this study. k_{entry} = kerf width entry (top) side, k_{exit} = kerf width exit (bottom) side, Z = focus position, N = nozzle stand-off position, θ = taper angle, HAZ = heat-affected zone, R_z = surface roughness, S = thickness of material. The dashed lines indicate the positions of the hardness measurements.